Wave Sequences For Solid Fuel In-Situ Combustion in Porous Media

A. J. DE SOUZA[1], I. Y. AKKUTLU[2], D. MARCHESIN[3]

[1] Departamento de Matemática e Estatística
Universidade Federal de Campina Grande
Av. Aprigio Veloso, 882, 58109-970, Campina Grande, PB, Brazil
E-mail:cido@dme.ufcg.edu.br

[2] Department of Civil and Environmental Engineering
University of Alberta
Edmonton, Alberta, Canada, T6G2G7
Email:yucel@ualberta.ca

[3] Instituto Nacional de Matemática Pura e Aplicada
Estrada Dona Castorina, 110, Jardim Botânico
22460-320 Rio de Janeiro, RJ, Brazil
Email: marchesi@fluid.impa.br

Abstract. We consider linear flow with forward combustion due to injection of air into a porous medium containing solid fuel. We neglect the gaseous phase compressibility and heat loss to the rock formation. Assuming that the combustion front is a traveling wave, we prove that there are only two possible time asymptotic wave sequences in the Riemann problem, depending on initial and injection conditions. One of the sequences consists of a thin region of cool unburned air, a warming shock wave with very slow speed, a hot region with unburned air, a combustion wave, a cool region with almost completely burned air, a gas composition wave, and a cool region without oxygen. The other sequence consists of a very thin region with unburned air at the injection temperature, a combustion wave, a hot region, a cooling thermal wave, a cool region, a gas composition wave and a cool region without oxygen. The waves in this problem have very different speeds, and therefore they cannot be observed in laboratory experiments that focus on the combustion wave. However, they do occur in field scale, so we analyze the Riemann solution for air injection with combustion.

Key words: combustion *in-situ*, porous media, Riemann solution.

AMS-subject classification: 80A25

Submitted to *Computational and Applied Mathematics*, 2004.
This work was supported in part by: CNPq under Grants 300204/83-3, 523258/95-0 and CNPq/PADCT 620017/2004-0; FINEP under CTPETRO Grant 21.01.0248.00; IM-AGIMP .

1. Introduction

Air injection and in-situ combustion have long been considered as a potential technique for displacement and recovery of heavy oil reserves [6, 11]. Operational advantage of this thermal recovery technique is the abundance of injection gas independent of location. It utilizes heavy and immobile components of the crude oil as fuel producing in-place heat necessary for the recovery of upgraded crude oil.

Despite the advantages and a long history, only a small fraction of the total thermal recovery corresponds to this technique. Some reasons are technical, such as the possibility of front extinction and the necessity of (re-)ignition for sustained propagation within in-situ combustion in the presence of external heat losses [1]. Thus the mathematical analysis of this problem is important to predict these events.

A large number of studies on the structure of the combustion front have been reported since 1950s. See [14, 10, 7, 9, 5, 12, 4, 1, 2, 3], for instance. These studies did not take into account other waves that occur in the combustion problem. As there is interaction between the combustion wave and other waves, this paper focuses on the solution of the Riemann problem with combustion, which takes into account all possible waves.

We assume that downstream processes during the in-situ combustion have already generated a stationary homogeneously distributed fuel. Burning of this fuel is the subject of the paper. A bimolecular reaction is assumed to take place between the injected oxygen and the solid fuel, hence the region of reaction behaves as a source of heat as well as a sink for both of the reactants. We consider uniform flow, transport and reaction of injected air in porous media of length l. We neglect external heat losses. We develop simplified theoretical models for forward (co-flow) combustion under varying boundary conditions and obtained the wave sequences in the Riemann solution. Formulation of the governing equations and the nomenclature follow the ones introduced by Akkutlu [1]. However, the reaction rate is further simplified for clarity in the context.

The paper is subdivided as follows. In Section (2) we derive the mathematical model. In Section (3) we determine the characteristic speeds and prove that all of them correspond to contact discontinuity shock waves. In Section (4) we introduce the combustion front as a traveling wave of the evolution system derived in Section (2). In this section we also discuss the Rankine-Hugoniot jump conditions for the combustion wave. In Section (5) we prove that for the physical parameters considered in this paper, there are no resonances between waves. As a consequence of this fact, we obtain two distinct temperature relationships for the combustion front, which we call the *hot upstream* and the *hot dowstream* combustion cases. Once these two cases are established we determine in Section (6) the ranges of parameters in which these combustion waves may exist. In Section (7) we present our main results concerning the possible wave sequences in the Riemann solution for the fuel deficient case behind the front combustion. In Theorem (7.1) we prove that for the hot upstream case, the wave sequence is uniquely determined under the temperature-controlled boundary condition ahead the combustion front. A similar result is proved in Theorem (7.4) for the hot downstream case. These cases occur for different injection-initial value conditions. We discuss the internal structure of noncombustion waves in Appendix (A), and the internal structure of the combustion wave in Appendix (B). Finally in Appendix (C) we present tables with typical values of parameters, constants and nomenclature used through the paper.

2. Formulation of the problem

We assume a 1-D geometry for the wave propagation. Conservation equations are written for the total energy and the total gas mass, and balance equations for the oxygen mass and the fuel mass. For the latter, we define the fuel density per total volume ρ_f and introduce the extent of conversion depth, $\eta(\tilde{x},\tilde{t}\,) = 1-\rho_f(\tilde{x},\tilde{t})/\rho_f^o$ (ρ_f^o is the initial fuel concentration), such that $\eta = 0$ corresponds to complete availability of fuel (denoted by superscript o) and $\eta = 1$ to the complete lack of fuel (the latter may occur because the fuel was never present or because it was completely consumed). The dependent variables are the temperature, $\tilde{T}(\tilde{x},\tilde{t}\,)$, the oxygen mass fraction, $\tilde{Y}(\tilde{x},\tilde{t}\,)$ and the fuel conversion depth $\eta(\tilde{x},\tilde{t}\,)$. The gas density $\rho_g(\tilde{T},\tilde{p}\,)$ is expressed by equation of state in terms of temperature and gas pressure $\tilde{p}(\tilde{x},\tilde{t}\,)$.

In formulating the conservation equations we make the following assumptions: the pore space and the solid matrix are in thermal equilibrium so that a one-temperature model is used for the energy balance; heat transfer by radiation, energy source terms due to pressure increase, and work from surface and body forces are all negligible; the ideal gas law is the equation of state for the gas phase; thermodynamic and transport properties, such as conductivity, diffusivity, heat capacity of the solid, heat of reaction, etc., all remain constant. We also neglect heat loss to the surrounding rock formation. The heat loss will be taken as zero as we study only the adiabatic case in this work. We assume that the pressure changes within any wave are negligible compared to the pressure drop across the system, so that in the ideal gas law and in other physical properties the pressure appears as a constant. Under these assumptions the dimensional form (superscript tilde) of the energy balance, the oxygen mass balance, the gaseous phase mass balance and the combustion kinetics equations are:

$$(1-\phi)\frac{\partial(c_s\rho_s\tilde{T})}{\partial\tilde{t}} + \frac{\partial(c_g\rho_g\tilde{v}\tilde{T})}{\partial\tilde{x}} = \tilde{\lambda}\frac{\partial^2\tilde{T}}{\partial\tilde{x}^2} + Q\rho_f^o W, \tag{2.1}$$

$$\frac{\partial(\phi\rho_g\tilde{Y})}{\partial\tilde{t}} + \frac{\partial(\rho_g\tilde{v}\tilde{Y})}{\partial\tilde{x}} = D_M\frac{\partial}{\partial\tilde{x}}\left(\rho_g\frac{\partial\tilde{Y}}{\partial\tilde{x}}\right) - \tilde{\mu}\rho_f^o W, \tag{2.2}$$

$$\frac{\partial(\phi\rho_g)}{\partial\tilde{t}} + \frac{\partial\,(\rho_g\tilde{v})}{\partial\tilde{x}} = \tilde{\mu}_g\rho_f^o W, \tag{2.3}$$

$$\frac{\partial\eta}{\partial\tilde{t}} = W, \tag{2.4}$$

where W is the rate of reaction. In the above, c_i denotes the average specific heat capacity of species i (gas or solid) at constant pressure, ρ_i is the volumetric density of species i, $\tilde{\lambda}$ is the effective thermal conductivity ($\tilde{\lambda}_s$=$\tilde{\lambda}_g$), Q is the heat of combustion, D_M is an effective diffusion coefficient in the gas phase (D=D_M/ϕ), while $\tilde{\mu} = \tilde{\gamma}M_o/M_f$ and $\tilde{\mu}_{gp} = \tilde{\gamma}_{gp}M_{gp}/M_f$ are mass-weighted stoichiometric coefficients for oxygen and for combustion gaseous products, respectively. The net gas mass production is determined from $\tilde{\mu}_g = \tilde{\mu}_{gp} - \tilde{\mu}$, so that positive or negative sign for $\tilde{\mu}_g$ correspond to net gaseous phase mass production or consumption, respectively. We will assume $\tilde{\mu}_g > 0$. For the rate of reaction, we use the first order law of mass action and a modified Arrhenius Law:

$$W = k(\tilde{T})\tilde{Y}\tilde{p}(1-\eta)\,, \quad \text{where}$$

$$k(\tilde{T}) = k_o e^{-E/R(\tilde{T}-\tilde{T}_{ig})}\,, \quad \text{for} \quad \tilde{T} > \tilde{T}_{ig}, \quad \text{and} \quad k(\tilde{T}) = 0\,, \quad \text{for} \quad \tilde{T} \le \tilde{T}_{ig},$$

with activation energy E and pre-exponential factor k_o. The temperature dependent exponential term in parenthesis ensures that the reaction rate is equal to zero at the ignition temperature $\tilde{T}_{ig} > 0$. In the standard Arrhenius law, $\tilde{T}_{ig} = 0$ K. In this work we will use $\tilde{T}_{ig} = \tilde{T}_0$, the reservoir temperature. This artificial T_{ig} is introduced to avoid technical problems related to the fact that the exponential factor becomes extremely small at ambient temperatures, but the formalism we use requires it to be zero to model complete extinction due to low temperature, [8].

We use the ideal gas equation of state $\tilde{p}M_g = \rho_g R\tilde{T}$.

Non-dimensionalized combustion equations. We introduce dimensionless space and time variables. To bring out the internal structure of the combustion wave, we introduce convenient variables and parameters that are defined in Section C.4. We scale the length by $l^*{=}\alpha_s/v^i$ and the time using $t^*{=}l^*/v^i$, where v^i is the injection velocity and α_s the effective thermal diffusivity. We introduce the scaled temperature $\theta = \tilde{T}/\tilde{T}_0$, which means that the reservoir temperature corresponds to $\theta_0 = 1$. Thus the equations (2.1)–(2.4) are transformed into the dimensionless balance equations

$$\frac{\partial\theta}{\partial\hat{t}} + \frac{\partial(a\rho v\theta)}{\partial\hat{x}} = \frac{\partial^2\theta}{\partial\hat{x}^2} + q\Phi, \tag{2.5}$$

$$\frac{\partial(\phi Y\rho)}{\partial\hat{t}} + \frac{\partial(\rho vY)}{\partial\hat{x}} = \frac{1}{L_e}\frac{\partial}{\partial\hat{x}}\left(\rho\frac{\partial Y}{\partial\hat{x}}\right) - \mu\Phi, \tag{2.6}$$

$$\phi\frac{\partial\rho}{\partial\hat{t}} + \frac{\partial(\rho v)}{\partial\hat{x}} = \mu_g\Phi, \tag{2.7}$$

$$\frac{\partial\eta}{\partial\hat{t}} = \Phi, \tag{2.8}$$

$$\rho\theta = 1, \tag{2.9}$$

where

$$\Phi = \alpha Y(1-\eta)\, e^{-\gamma/(\theta-1)}, \quad \text{for } \theta > 1, \quad \text{and} \quad \Phi = 0, \quad \text{for } \theta \le 1. \tag{2.10}$$

The domain of the dependent variables is given by

$$\theta \ge 0, \quad 0 \le Y \le 1, \quad 0 \le \eta \le 1, \quad v > 0. \tag{2.11}$$

From now on, we write $\hat{t} \to t$, $\hat{x} \to x$.

3. Non-combustion waves for the model in hyperbolic framework

In the absence of combustion, the terms containing the factor Φ vanish in the right hand sides of system (2.5)–(2.9). Of course Φ vanishes for $Y \equiv 0$, or $\eta \equiv 1$, or $\theta \le 1$. Even though it is not essential, we take the shortcut of neglecting the second derivative terms, in order to be in the hyperbolic framework and focus the waves for large times and long distances. Assuming for the time being smoothness of solutions we can expand the derivatives in the

remaining terms in Eqs. (2.5-2.8), manipulate Eqs. (2.6), (2.7), use Eq. (2.9) to eliminate ρ, obtaining:

$$\frac{\partial \theta}{\partial t} + a\frac{\partial v}{\partial x} = 0, \tag{3.1}$$

$$\phi\frac{\partial Y}{\partial t} + v\frac{\partial Y}{\partial x} = 0, \tag{3.2}$$

$$\left(\frac{\theta}{a} + \phi\right)\frac{\partial \theta}{\partial t} + v\frac{\partial \theta}{\partial x} = 0, \tag{3.3}$$

$$\frac{\partial \eta}{\partial t} = 0. \tag{3.4}$$

The characteristic speeds of system (3.1-3.4) in increasing order and the corresponding characteristic vectors are

$$\lambda^\eta = 0, \qquad (0,0,1,0)^T, \tag{3.5}$$

$$\lambda^\theta = a\,\frac{v}{\theta + a\phi}, \qquad a\,(1,0,0,\frac{v}{\theta + a\phi})^T, \tag{3.6}$$

$$\lambda^Y = v/\phi, \qquad (0,1,0,0)^T. \tag{3.7}$$

It is easy to see that all characteristic speeds are constant along the integral curves defined by the corresponding characteristic vector fields, which means that all of them are associated to contact discontinuities, hence they satisfy the Rankine-Hugoniot conditions for (3.1)-(3.4), [13]. The characteristic speed λ^η corresponds to an immobile discontinuity along which only η varies, λ^θ corresponds to a thermal discontinuity along which θ and v vary and λ^Y corresponds to a gas composition discontinuity along which only Y varies.

4. Combustion wave

We proceed next with the study of combustion wave propagation, which occurs for $\theta > 1$ (see Eq. (2.10)). The combustion front connects *burned states* behind of it, denoted by $U^b \equiv (\theta^b, Y^b, \eta^b, v^b)$, to *unburned states* ahead of it, denoted by $U^u \equiv (\theta^u, Y^u, \eta^u, v^u)$.

We look for combustion fronts as steady traveling waves of system (2.5)-(2.10) with propagation speed $V > 0$ by setting $x = \hat{x} - V\hat{t}$ and $t = \hat{t}$. In these moving nondimensional coordinates, after using Eq. (2.9) to eliminate ρ, the equations (2.5)-(2.8) read, after writing $\hat{t} \to t$, $\hat{x} \to x$:

$$\frac{d}{dx}\,(av - V\theta) = \frac{d^2\theta}{dx^2} - q\frac{d(V\eta)}{dx}, \tag{4.1}$$

$$\frac{d}{dx}\left(\frac{1}{\theta}(v - \phi V)Y\right) = \frac{1}{L_e}\frac{d}{dx}\left(\frac{1}{\theta}\frac{dY}{dx}\right) + \mu\frac{d(V\eta)}{dx}, \tag{4.2}$$

$$\frac{d}{dx}\left(\frac{1}{\theta}(v - \phi V)\right) = -\mu_g\frac{d(V\eta)}{dx}, \tag{4.3}$$

$$\frac{d(V\eta)}{dx} = -\Phi. \tag{4.4}$$

In the following, we consider the fuel-deficient case under three different conditions ahead of the combustion wave at $x = +\infty$: (1) the case where combustion wave ahead is temperature-controlled; (2) the limit case of (1) with complete consumption of oxygen; and (3) complete oxygen consumption not temperature-controlled. These conditions can be summarized as

$$(1) \quad \theta = \theta^u = 1, \quad Y = Y^u > 0, \quad \eta = \eta^u = 0, \quad v = v^u > 0; \quad x \to +\infty, \tag{4.5}$$

$$(2) \quad \theta = \theta^u = 1, \quad Y = Y^u = 0, \quad \eta = \eta^u = 0, \quad v = v^u > 0; \quad x \to +\infty. \tag{4.6}$$

$$(3) \quad \theta = \theta^u > 1, \quad Y = Y^u = 0, \quad \eta = \eta^u = 0, \quad v = v^u > 0; \quad x \to +\infty, \tag{4.7}$$

In the adiabatic case studied here, reaction at the back of the combustion zone ceases due to complete lack of fuel. This means that there is complete consumption of the fuel behind (i.e., η^b=1 at $-\infty$). Since gas is continuously injected we have $Y^b = 1$. The temperature and the velocity behind the combustion need to be calculated. Thus the boundary conditions behind the combustion front are generically given by:

$$\theta = \theta^b > 0, \quad Y = Y^b = 1, \quad \eta = \eta^b = 1, \quad v = v^b > 0; \quad x \to -\infty\,. \tag{4.8}$$

Integrating equations (4.1)-(4.3) from x to $+\infty$ once, taking into account that $\eta^u = 0$ at $x = +\infty$ and re-ordering, we get

$$\frac{d\theta}{dx} = a(v - v^u) - V(\theta - \theta^u) + q\eta, \tag{4.9}$$

$$\frac{dY}{dx} = L_e\theta\left(\frac{1}{\theta}(v - \phi V)Y - \frac{1}{\theta^u}(v^u - \phi V)Y^u - \mu V\eta\right), \tag{4.10}$$

$$\frac{1}{\theta}(v - \phi V) - \frac{1}{\theta^u}(v^u - \phi V) + \mu_g V\eta = 0, \tag{4.11}$$

$$V\frac{d\eta}{dx} = -\Phi. \tag{4.12}$$

Next, we substitute the value of v given by equation (4.11) into (4.9) and (4.10), and substitute the value of Φ given by Eq. (2.10) into (4.12) to obtain the reduced system:

$$\frac{d\theta}{dx} = a\left(\frac{v^u\theta}{\theta^u} - \big((\frac{\theta}{\theta^u} - 1)\phi + \mu_g\eta\theta\big)V - v^u\right) - V(\theta - \theta^u - q\eta), \tag{4.13}$$

$$\frac{dY}{dx} = L_e\theta\left(\big(\frac{v^u}{\theta^u} - (\frac{\phi}{\theta^u} + \mu_g\eta)V\big)Y - \mu V\eta - \frac{1}{\theta^u}\big(v^u - \phi V\big)Y^u\right), \tag{4.14}$$

$$\frac{d\eta}{dx} = -\frac{\alpha}{V}Y\,(1 - \eta)\,e^{-\gamma/(\theta-1)}, \quad \text{for } \theta > 1, \quad \text{and} \quad \frac{d\eta}{dx} = 0\,, \quad \text{for } \theta \le 1. \tag{4.15}$$

We want to know if there is a solution of the reduced system (4.13)-(4.15) for any one of the boundary conditions (4.5)-(4.7) together with (4.8) connecting the burned state $U^b \equiv (\theta^b, Y^b, \eta^b; v^b)$ at $x \to -\infty$ to the unburned state $U^u \equiv (\theta^u, Y^u, \eta^u; v^u)$ and $x \to +\infty$. If it exists, such solution represents the profile of a traveling wave connecting the burned state to the unburned state. As a preliminary step to establish its existence, the Rankine-Hugoniot condition relating the burned and unburned states is considered in the next subsection.

4.1. **The Rankine-Hugoniot equations for combustion.** For the boundary conditions given in (4.8) at $-\infty$ and in (4.5)-(4.7) at $+\infty$, taking into account that $\partial\theta/\partial x$, $\partial Y/\partial x$ and

$\partial\theta/\partial x$ tend to zero as x tends to $\pm\infty$, the R.H.S. of equations (4.13)-(4.14) become

$$a\left(\frac{v^u\theta^b}{\theta^u}-\left((\frac{\theta^b}{\theta^u}-1)\phi+\mu_g\theta^b\right)V-v^u\right)-V(\theta^b-\theta^u-q)=0\,, \tag{4.16}$$

$$L_e\theta^b\left(\frac{v^u}{\theta^u}-(\frac{\phi}{\theta^u}+\mu+\mu_g)V-\frac{1}{\theta^u}(v^u-\phi V)Y^u\right)=0\,, \tag{4.17}$$

and Eq. (4.15) becomes a trivial identity. Taking $x\to-\infty$ in Eq. (4.11) we obtain a separate equation for v^b:

$$v^b-\phi V=\left(\frac{1}{\theta^u}(v^u-\phi V)-\mu_g V\right)\theta^b. \tag{4.18}$$

Equations (4.16)-(4.18) are the Rankine-Hugoniot conditions relating the combustion front speed V and the unburned and burned states ahead and behind the combustion wave.

4.2. **Solutions of the Rankine-Hugoniot equations.** The solutions of the Rankine Hugoniot equations (4.16) and (4.17) for a fixed value $\theta^u\geq 1$ are obtained now. Since λ^Y is the particle speed of gas it is convenient to introduce the variable $V^u(V,v^u)\equiv V/\lambda^Y(U^u)$ given by

$$V^u=\phi V/v^u\,. \tag{4.19}$$

Equations (4.16) and (4.17) give θ^b and Y^u respectively in terms of V, v^u and θ^u, or in terms of V^u and θ^u as follows:

$$\theta^b=\frac{((\theta^u+q+a\phi)V-av^u)\,\theta^u}{((1+a\mu_g)\theta^u+a\phi)\,V-av^u}\,,\quad\text{or}\quad \theta^b=\frac{((\theta^u+q+a\phi)V^u-a\phi)\,\theta^u}{((1+a\mu_g)\theta^u+a\phi)\,V^u-a\phi}\,, \tag{4.20}$$

$$Y^u=\frac{v^u-(\phi+(\mu_g+\mu)\theta^u)\,V}{v^u-\phi V}\,,\quad\text{or}\quad Y^u=\frac{\phi-(\phi+(\mu_g+\mu)\theta^u)\,V^u}{\phi(1-V^u)}\,. \tag{4.21}$$

For a fixed value of θ^u, Eq. (4.20b) represents θ^b in terms of V^u as a hyperbola drawn schematically in Fig. (4.1), constructed for the parameter range in Table I. This hyperbola has vertical and horizontal asymptotes respectively at

$$V^u_d=\frac{a\phi}{(1+a\mu_g)\theta^u+a\phi}\,,\qquad \theta^b_a=\frac{(\theta^u+q+a\phi)\theta^u}{(1+a\mu_g)\theta^u+a\phi}\,. \tag{4.22}$$

The intersections of the hyperbola with the horizontal and vertical coordinate axes occur at

$$\theta^b=\theta^u,\quad\text{and}\quad V^u_n=\frac{a\phi}{\theta^u+q+a\phi}\,. \tag{4.23}$$

Notice that since $a\mu_g<q$ from Eqs. (4.22) and (4.23) we see that $\theta^b_a>\theta^u$ and $V^u_n<V^u_d<1$, respectively.

Remark 4.1. The constants V^u_p and $\theta^b_p=\theta^b(V^u_p)$ in Fig. (4.2) are related to Eq. (4.21b) and will be explained in the text. The constant θ_M is calculated in (5.1) and $V^u_M=V^u(\theta_M)$ is obtained from (4.28).

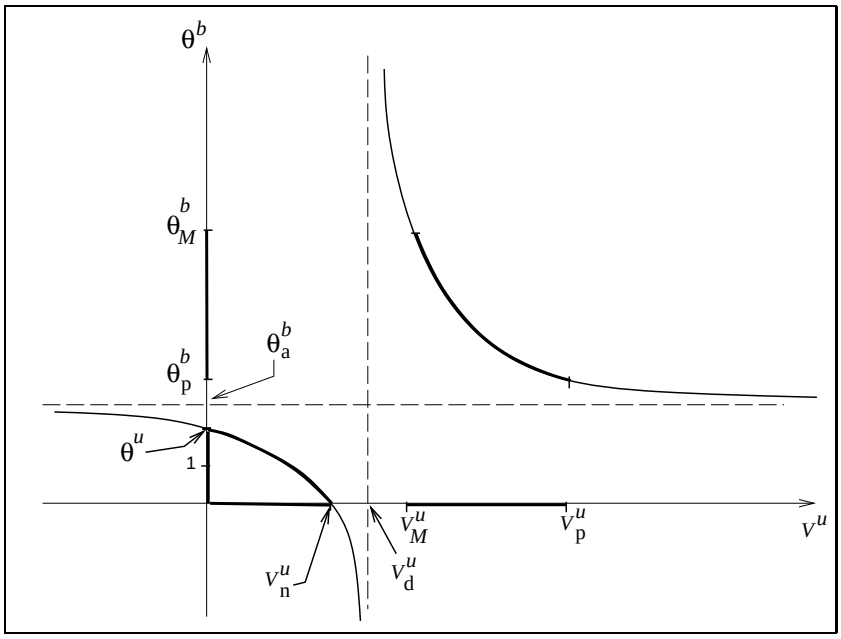

FIGURE 4.1. θ^b as a function of V^u given by (4.20b).

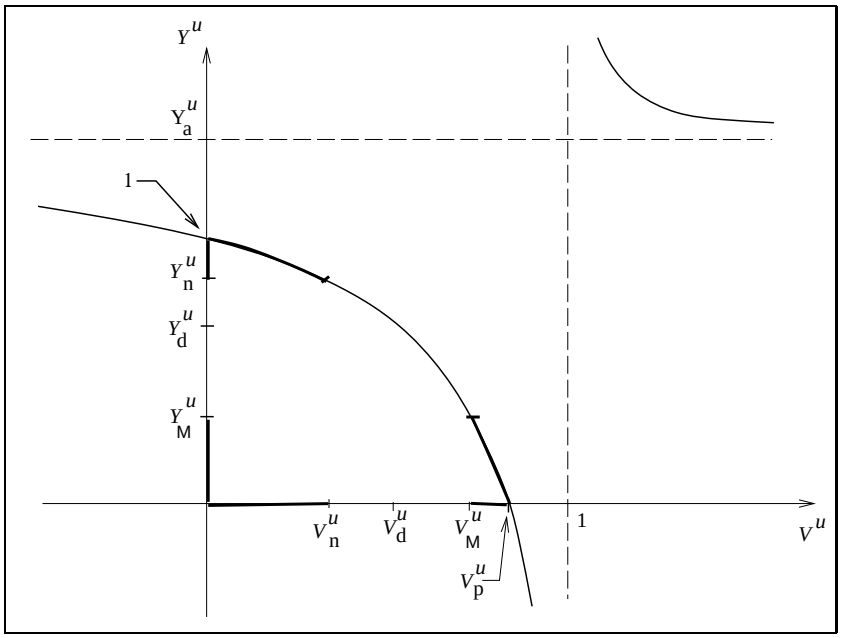

FIGURE 4.2. Y^u as a function of V^u given by (4.21b).

Now let us consider Eq. (4.21b) for a fixed value of $\theta^u \geq 1$. This equation represents Y^u in terms of V^u as a hyperbola, which is drawn schematically in Fig. (4.2). This hyperbola has vertical asymptote $V^u = 1$ and horizontal asymptote at $Y^u = \phi + \theta^u(\mu + \mu_g)/\phi$ (denoted by Y^u_a in (4.2)), which has no physical meaning.

The intersections of the hyperbola with the horizontal and vertical coordinate axes occur at

$$Y^u = 1\,, \quad \text{and} \quad V_p^u = \frac{\phi}{\phi + \theta^u(\mu + \mu_g)}\,. \tag{4.24}$$

Notice that $V_p^u = 1/Y_a^u < 1$.

Remark 4.2. For the quantities in Figs. (4.1) and (4.2), corresponding to the parameters in Table I, the inequalities $0 < V_n^u < V_d^u < V_M^u < V_p^u < 1$ hold.

It is also possible to express θ^b in terms of θ^u and V^b, where

$$V^b \equiv V/\lambda^Y(U^b) = \phi V/v^b\,, \tag{4.25}$$

as follows. Using Eq. (4.18) we obtain

$$v^u = \frac{1}{\theta^b}\left(\theta^u v^b + \big((\theta^b - \theta^u)\phi + \mu_g\theta^u\theta^b\big)V\right). \tag{4.26}$$

Substituting equation (4.26) into equation (4.20b) gives

$$V^b(\theta^b)^2 + \big(a(\phi V^b - \phi + \mu_g\theta^u V^b) - (\theta^u + q)V^b\big)\theta^b + a\phi\theta^u(1 - V^b) = 0\,. \tag{4.27}$$

Alternatively, instead of obtaining an expression for θ^b as a function of V^u and θ^u as in (4.20b), Eq. (4.16) could be utilized to find V^u as function of θ^b and θ^u:

$$V^u = \frac{a\phi(\theta^u - \theta^b)}{(\theta^u)^2 - \left((\theta^b - q) - a(\phi - \mu_g\theta^b)\right)\theta^u - a\phi\theta^b}\,. \tag{4.28}$$

Similarly V^b can be written in terms of θ^b:

$$V^b = \frac{a\phi(\theta^b - \theta^u)}{(\theta^b)^2 - \big((\theta^u + q) - a(\phi + \mu_g\theta^u)\big)\theta^b - a\phi\theta^u}. \tag{4.29}$$

The graph defined by Eq. (4.29) is schematically drawn in Fig. (4.3). Direct calculations show that the denominator in Eq. (4.29) possesses two real roots θ_1^b and θ_2^b, with $\theta_1^b < 0$ and $\theta_2^b > \theta^u \geq 1$. Thus the graph of Eq. (4.29) possesses vertical asymptotes given by $\theta^b = \theta_1^b$ and $\theta^b = \theta_2^b$. The graph possesses also a horizontal asymptote given by $V^b = 0$.

Since we are interested in forward combustion we have that $V > 0$. From Eqs. (4.19) and (4.25) it follows that $V^u > 0$ and $V^b > 0$. Thus, only the portions of the graphs in Figs (4.1), (4.2) and (4.3) in the first quadrant must be considered. With this in mind we conclude that the following restrictions hold:

$$0 < V^u < V_n^u\,, \quad \text{or} \quad V_d^u < V^u \leq V_p^u\,, \tag{4.30}$$

$$0 \leq \theta^b < \theta^u\,, \quad \text{or} \quad \theta^b \geq \theta_p^b > \theta^u\,, \tag{4.31}$$

$$0 < V^b < 1\,. \tag{4.32}$$

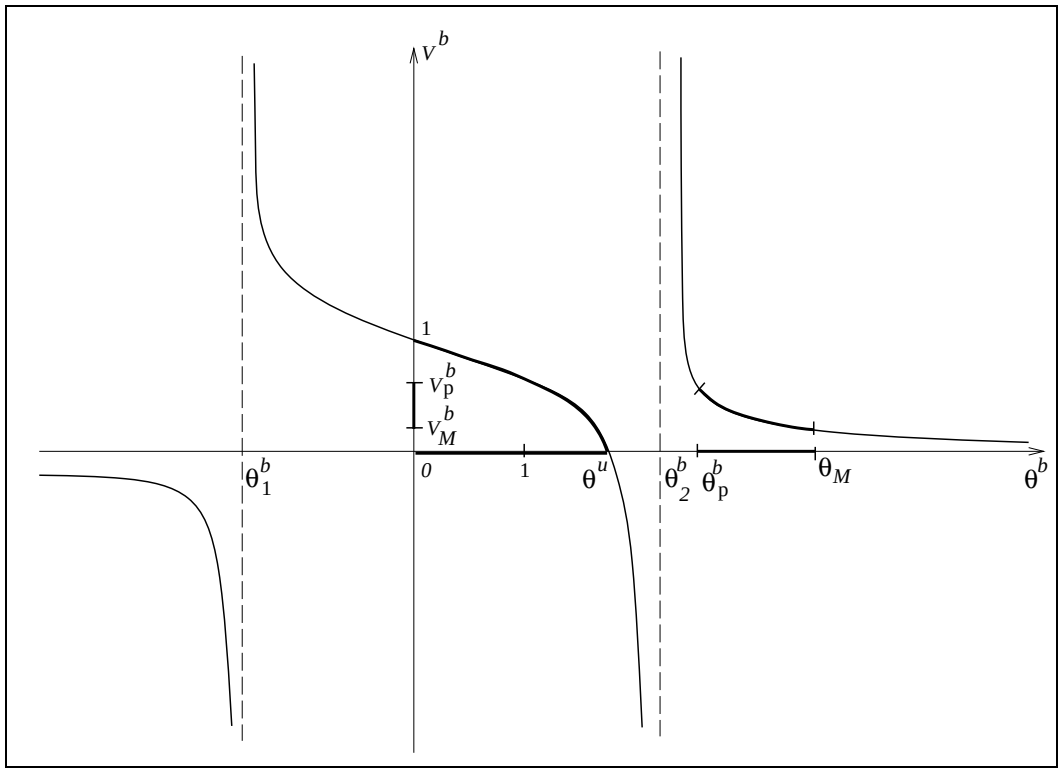

FIGURE 4.3. $V^b\big(\theta^b\big)$ defined by equation (4.29).

5. Absence of wave resonances

We can expect that changes of wave structure in the combustion Riemann problem occur whenever two wave speeds coincide, either in the burned or in the unburned regions. Such changes are ruled out by the following theorem about resonances, plus some physical considerations.

Theorem 5.1. *Consider $U = (\theta, Y, \eta, v)$ in the physical domain defined Eq. (2.11).*
(a) The non-combustion waves have distinct speeds.
(b) The combustion, the immobile and the gas composition waves have distinct speeds.
(c) The combustion and the thermal waves have the same speed if, and only if, $\theta^b = \theta_M$, or $\theta^u = \theta_M$, where

$$\theta_M = \frac{q}{a\mu_g}\,. \tag{5.1}$$

Proof. (a) From equations (3.5)–(3.7), we obtain explicitly that

$$\lambda^\eta < \lambda^\theta < \lambda^Y\,, \qquad \text{everywhere}, \tag{5.2}$$

which means that there are no speed equalities among the non-combustion waves.
(b) Since we are considering forward combustion there is no resonance between the combustion and the immobile wave.

From Eqs. (4.30) and (4.32), we have that $0 < V^u < 1$ and $0 < V^b < 1$, respectively. Since $V^u = V/\lambda^Y(U^u)$ and $V^b = V/\lambda^Y(U^b)$, it follows respectively that

$$V < \lambda^Y(U^u) \quad \text{ and } V < \lambda^Y(U^b)\,. \tag{5.3}$$

(c) Since the thermal wave is a contact discontinuity, the combustion speed V coincides with λ^θ if and only if:

$$V = \lambda^\theta(U^b) = \lambda^\theta(U^u)\,. \tag{5.4}$$

From Eqs. (3.6), (4.25) and (4.29), we have that

$$\begin{aligned} V =&\lambda^\theta(U^b) \quad \text{if, and only if} \quad V^b = \frac{a\,\phi}{\theta^b + a\phi} \quad \text{if, and only if} \\ &\frac{(\theta^b - \theta^u)}{(\theta^b)^2 - ((\theta^u + q) - a(\phi + \mu_g\theta^u))\,\theta^b - a\phi\theta^u} = \frac{1}{\theta^b + a\phi} \quad \text{if, and only if} \\ &\theta^b(a\mu_g\theta^u - q) = 0 \quad \text{if, and only if} \quad \theta^u = \theta_M\,. \end{aligned} \tag{5.5}$$

From Eqs. (3.6), (4.19) and (4.28) we have that

$$\begin{aligned} V =&\lambda^\theta(U^u) \quad \text{if, and only if} \quad V^u = \frac{a\,\phi}{\theta^u + a\phi} \quad \text{if, and only if} \\ &\frac{(\theta^u - \theta^b)}{(\theta^u)^2 - ((\theta^b - q) - a(\phi - \mu_g\theta^b))\,\theta^u - a\phi\theta^b} = \frac{1}{\theta^u + a\phi} \quad \text{if, and only if} \\ &\theta^u(a\mu_g\theta^b - q) = 0 \quad \text{if, and only if} \quad \theta^b = \theta_M\,. \end{aligned} \tag{5.6}$$

The proof is complete.

Remark 5.2. Direct calculations with the value of the parameters in Table I give us $\theta_M \approx 24.21264641$. This corresponds to an extremely large temperature value above 6000 K that is beyond physical interest. Thus this value of θ_M defines a maximum value for the range of θ, and below this value there are no speed coincidences.

Since V^u and V^b are both positive from Eqs. (5.5) and (5.6), we see that the sign of $(\theta^b - \theta^u)$ determines if $V < \lambda^\theta$ or $V > \lambda^\theta$.

Thus, given $\theta^u \geq 1$, we are led to the following two possible temperature relationships for the combustion front:

$$(A) \quad \text{Hot downstream} \qquad \theta^b > \theta^u, \quad \text{for} \quad V > \lambda^\theta(U^b) \text{ and } V > \lambda^\theta(U^u)\,; \tag{5.7}$$

$$(B) \quad \text{Hot upstream} \quad 0 \leq \theta^b < \theta^u, \quad \text{for} \quad V < \lambda^\theta(U^b) \text{ and } V < \lambda^\theta(U^u)\,. \tag{5.8}$$

6. The admissible Rankine-Hugoniot locus for the combustion wave

Cases (A) and (B) in (5.7) and (5.8) give distinct possibilities for the admissible combustion wave depending on the variable θ^b, Y^b, V^u and V^b sketched in Figs. (4.1), (4.2) and (4.3) as will be discussed in the next two subsections.

6.1. **Hot Dowstream.** Since $\theta^b > \theta^u$ (see Fig. (4.1)) it follows that $V^u > V^u_d$. Since $0 \leq Y^b \leq 1$ (see Fig. (4.2)) it follows that $V^u \leq V^u_p$.

Let $V^u_M = V^u(\theta_M)$ in Fig. (4.1) obtained from Eq. (4.28), where θ_M is the maximum value for the nondimensionalized temperature θ defined in (5.1). In the same way, let $V^b_M = V^b(\theta_M)$ and $V^b_p = V^b(\theta^b_p)$ in Fig (4.3) obtained from Eq. (4.29). Finally, let $Y^u_M = Y^u(V^u_M)$ in Fig. (4.2) obtained from Eq. (4.21b).

Comparing Figs. (4.1), (4.2) and (4.3), we conclude that in case (A), for a fixed value of $\theta^u \geq 1$, the admissible values of θ^b, V^b, V^u and Y^u vary in the ranges:

$$\theta_p^b \leq \theta^b < \theta_M\,, \quad \text{(see Figs. (4.1), (4.3))}, \tag{6.1}$$

$$V_M^b < V^b \leq V_p^b\,, \quad \text{(see Fig. (4.3))}, \tag{6.2}$$

$$V_M^u < V^u \leq V_p^u\,, \quad \text{(see Figs. (4.1), (4.2))}, \tag{6.3}$$

$$0 \leq Y^u < Y_M^u\,, \quad \text{(see Fig. (4.2))}. \tag{6.4}$$

6.2. **Hot Upstream.** Since $0 \leq \theta^b < \theta^u$ we see that $0 < V^u \leq V_n^u$, where V_n^u was defined in (4.23). See Fig. (4.1).

Let $Y_n^u = Y^u(V_n^u)$ in Fig.(4.2) obtained from Eq. (4.21b). Since $0 < V^u \leq V_n^u$ it follows that $Y_n^u \leq Y^u < 1$.

Since $0 \leq \theta^b < \theta^u$, from Fig. (4.3), it follows that $0 < V^b \leq 1$.

Thus in *Case (B)*, for a fixed value of $\theta^u \geq 1$, the values of θ^b, V^b, V^u and Y^u vary in the ranges:

$$0 \leq \theta^b < \theta^u\,, \text{ (see Figs. (4.1), (4.3))}, \tag{6.5}$$

$$0 < V^b \leq 1\,, \quad \text{(see Fig. (4.3))}, \tag{6.6}$$

$$0 < V^u \leq V_n^u\,, \quad \text{(see Figs. (4.1), (4.2))}, \tag{6.7}$$

$$Y_n^u \leq Y^u < 1\,, \quad \text{(see Fig. (4.2))}. \tag{6.8}$$

7. Wave sequences in the Riemann solutions

We have completed in Section (5) the proof that there is no wave speed coincidence in combustion problems with incomplete oxygen consumption for temperatures of physical interest. We also have determined the admissible ranges of the main parameters along the Hugoniot-locus in Section (6). According to the discussion in Section (B) we will assume the existence of a traveling wave profile representing the combustion front for parameters in the ranges (6.1)-(6.4) and (6.5)-(6.8). Under this assumption, for any fixed value of $\theta^u \geq 1$, we are able to obtain the description of the wave sequence in the Riemann solution for cases (A) or (B) defined in (5.7) or (5.8).

7.1. **Hot upstream combustion.** In this case the wave sequence in the Riemann solution may be at most a (perhaps trivial) immobile fuel shock, a thermal shock with speed λ^θ, a combustion front with speed V, and a gas composition shock with speed λ^Y, depending on the boundary condition ahead of the combustion front.

We denote this sequence of waves, represented in Fig. (7.1) by means of the following convention:

$$U^i \xrightarrow{\lambda^\eta} U_1 \xrightarrow{\lambda^\theta} U^b \xrightarrow{V} U^u \xrightarrow{\lambda^Y} U_0\,. \tag{7.1}$$

The state $U^i = (\theta^i, 1, 0, v^i)$ denotes the injection conditions, $U_1 = (\theta^i, 1, 1, v^i)$ denotes an intermediate state in the burned region, $U^b = (\theta^b, 1, 1, v^b)$ and $U^u = (1, Y^u, 0, v_0)$ are the burned and the unburned states surrounding the combustion front and $U_0 = (1, 0, 0, v_0)$ denotes the reservoir conditions at the production. The values of θ^i and v^i are given, but the speeds λ^θ, V, λ^Y and the values of θ^b, v^b, Y^u and v_0 have to be determined.

We have the following

Theorem 7.1. *Given the injection conditions* $U^i = (\theta^i, 1, 0, v^i)$ *and the value of* $V^u \in (V_M^u, V_p^u)$*, assume that in the hot upstream combustion case (A) defined in (5.7) a combustion wave is present in the wave sequence for the Riemann solution of (2.5)-(2.10), with parameters in the ranges given in Eqs. (6.1)-(6.4). Then the wave sequence in (7.1) is uniquely determined for the boundary conditions (4.5) and (4.8).*

Proof. Inspecting Fig. 7.1, we see that if the injection rate v^i, the temperature θ^i and the value of V^u are given, then the speeds λ^θ, V and λ^Y in the wave sequence (7.1) and the values of θ^b, v^b, Y^u, v^u and v_0 are determined as follows.

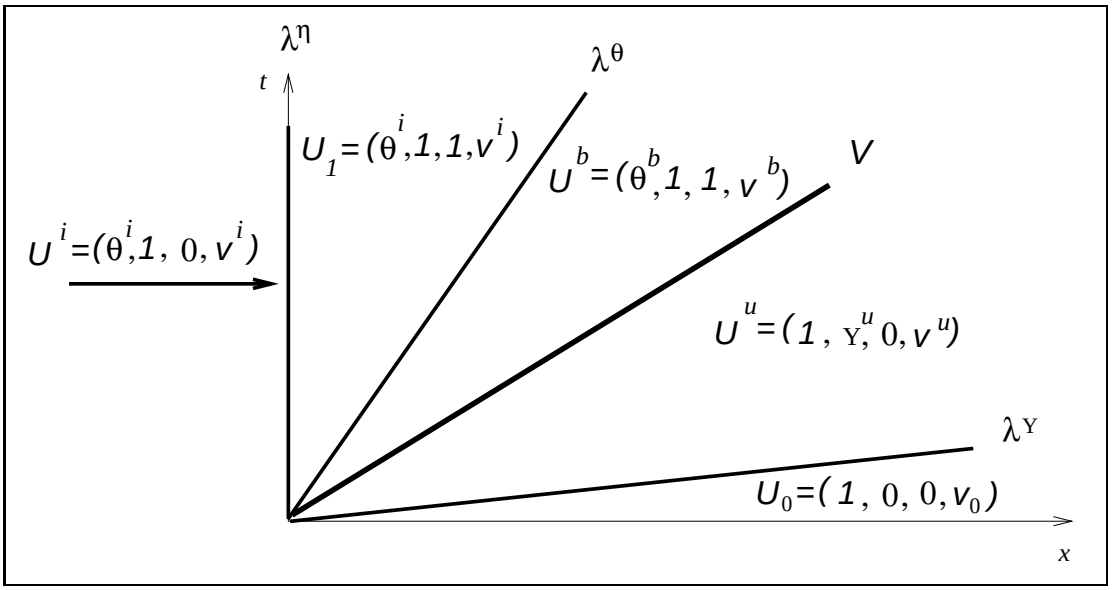

FIGURE 7.1. *Case (A.1):* Regions separated by immobile, thermal, combustion and gas composition waves. Values of θ, Y, η and v in each region. The latter region is actually very thin.

From Eq. (3.6), we have:

$$\lambda^\theta = \frac{av^i}{\theta^i + a\phi}, \qquad \text{(so } \lambda^\theta \text{ is determined already).}$$

From Eq. (4.20b) with $\theta^u = 1$, we have

$$\theta^b = \frac{(1 + q + a\phi)V^u - a\phi}{(1 + a\mu_g + a\phi)\, V^u - a\phi}\,.$$

Since the thermal wave is a contact discontinuity, it follows that:

$$v^b = \frac{\theta^b + a\phi}{\theta^i + a\phi}\, v^i\,.$$

From Eq. (4.29) with $\theta^u = 1$, we have

$$V^b = \frac{a\phi(\theta^b - 1)}{(\theta^b)^2 - \big((1+q) - a(\phi + \mu_g)\big)\theta^b - a\phi}.$$

From Eq. (4.25) we obtain the combustion speed V; then we obtain v^u from Eq. (4.19). From Eq. (4.21b) with $\theta^u = 1$, we obtain Y^u and from Eq. (3.7) with $v = v^u$, we obtain the value of λ^Y:

$$V = v^b V^b/\phi\,,$$

$$v^u = \phi V/V^u\,,$$

$$Y^u = \frac{\phi - (\phi + \mu_g + \mu)\, V^u}{\phi(1 - V^u)}\,,$$

$$\lambda^Y = v^u/\phi\,.$$

Finally, since the gas composition wave is a contact discontinuity it follows that

$$v_0 = v^u\,,$$

which provides a consistent solution of the system of conservation laws in the hyperbolic framework for the boundary conditions (4.5) and (4.8). This completes the proof of the Theorem (7.1).

Remark 7.2. Theorem (7.1) can be extended to the limit case (2) in Eq. (4.6) of complete oxygen consumption and controlled-temperature ahead the combustion: $\theta^u = 1$, $Y^u = 0$, $\eta^u = 0$, $v^u = v_0 > 0$. See Fig. (7.2).

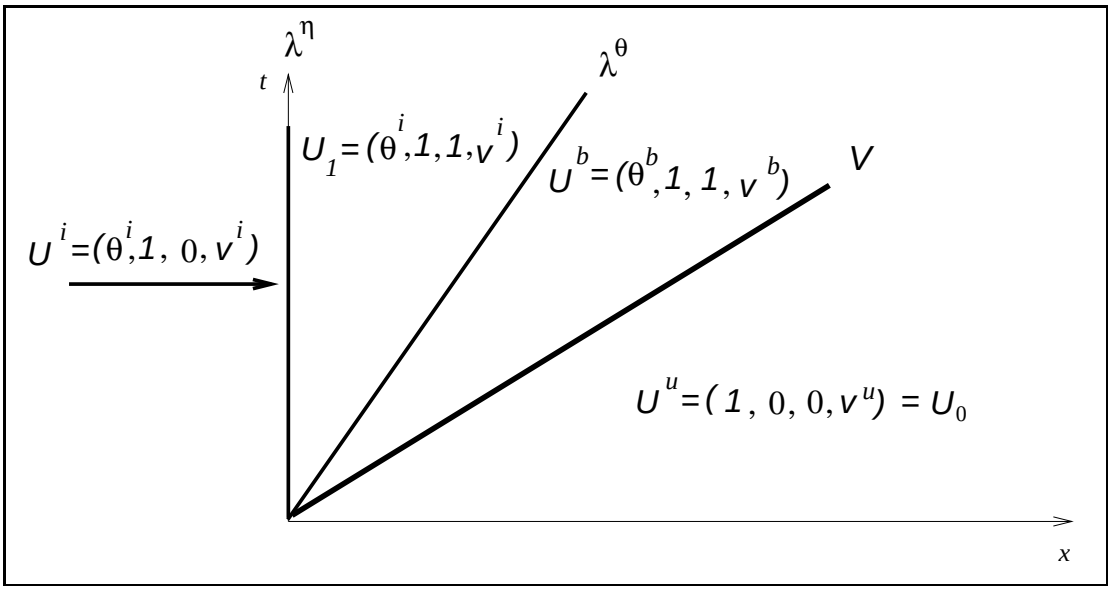

FIGURE 7.2. *Case (A.2):* Regions separated by immobile, thermal wave and combustion waves. Values of θ, Y, η and v in each region.

Since θ^u is given, it is not necessary to give the parameter V^u because from Eq. (4.21b) with $\theta^u = 1$ and $Y^u = 0$, it follows that $V^u = V_p^u$, where V_p^u is defined in Eq. (4.24) (see

Fig. (4.2)). Since $Y^u = 0$, the strength of the gas composition wave is zero. From Eq. (4.20b) with $\theta^u = 1$ and $V^u = V_p^u$, it follows that

$$\theta^b = \frac{(1+q+a\phi)V_p^u - a\phi}{(1+a\mu_g+a\phi)V_p^u - a\phi} \equiv \theta_p^b\,, \quad \text{(see Fig. (4.1))}. \tag{7.2}$$

The values of the thermal shock speed λ^θ, v^b, the combustion front speed V and v_0 are obtained through the same procedure used in the proof of Theorem (7.1).

Remark 7.3. We remark that the case (3) given by Eq. (4.7) is inconsistent with the hot upstream case (A) due to the restrictions in Eq. (5.7) that $V > \lambda^\theta(U^u) = \lambda^\theta$. If $\theta^u > 1$, then there should be another thermal wave ahead the combustion front, where the temperature decreases from $\theta = \theta^u$ to $\theta_0 = 1$, contradicting the conditions in Eq. (5.7).

7.2. **Hot downstream combustion.** Recall that in the downstream combustion case we have to restrict the parameters to the ranges defined by Eqs. (6.5)–(6.8). Since $0 < Y_n^u < Y^u < 1$ complete oxygen consumption (as stated in case (2) defined by Eq. (4.6) and case (3) defined by Eq. (4.7)) is impossible.

For the temperature-controlled case in (4.5) we have that $\theta^u = 1$, the reservoir temperature. Since the combustion front is the first non immobile wave, it follows that the thermal wave possesses zero strenght. See Fig. (7.3)

Thus we have the following wave sequence represented in Fig. (7.3):

$$U^i \xrightarrow{\lambda^\eta} U^b \xrightarrow{V} U^u \xrightarrow{\lambda^Y} U_0\,, \tag{7.3}$$

where the state $U^i = (\theta^i, 1, 0, v^i)$ denotes the injection conditions, $U^b = (\theta^i, 1, 1, v^i)$ and $U^u = (1, Y^u, 0, v^u)$ define the burned and the unburned states surrounding the combustion front, respectively, and $U_0 = (1, 0, 0, v_0)$ denotes the reservoir conditions at the production. The values of θ^i, v^i and v^u are given, but the speeds V, and λ^Y as well as the value of Y^u have to de determined.

We have the following

Theorem 7.4. *Given the injection conditions $U^i = (\theta^i,\ 1,\ 0,\ v^i)$ and the velocity v^u ahead of the combustion front, assume that in the hot downstream combustion case (B) defined in (5.8) a combustion wave is present in the wave sequence for the Riemann solution of (2.5)-(2.10), with parameters in the ranges given in Eqs. (6.5)-(6.8). Then the wave sequence in (7.3) is uniquely determined for the boundary conditions (4.5) and (4.8).*

Proof. From Eq. (3.7), we obtain the gas composition shock speed:

$$\lambda^Y = v^u/\phi = v_0/\phi\,. \quad \text{Thus } v_0 = v^u.$$

From Eq. (4.18) with $\theta^b = \theta^i$, $v^b = v^i$ and $\theta^u = 1$, the value of the combustion front speed is given by:

$$V = \frac{v^i - v^u\theta^i}{\phi(1-\theta^i) - \mu_g\theta^i}\,.$$

From Eq. (4.21a) with $\theta^u = 1$, we obtain the value of Y^u as:

$$Y^u = \frac{v^u - (\phi + \mu_g + \mu)V}{v^u - \phi V}\,,$$

which concludes the proof of Theorem (7.4).

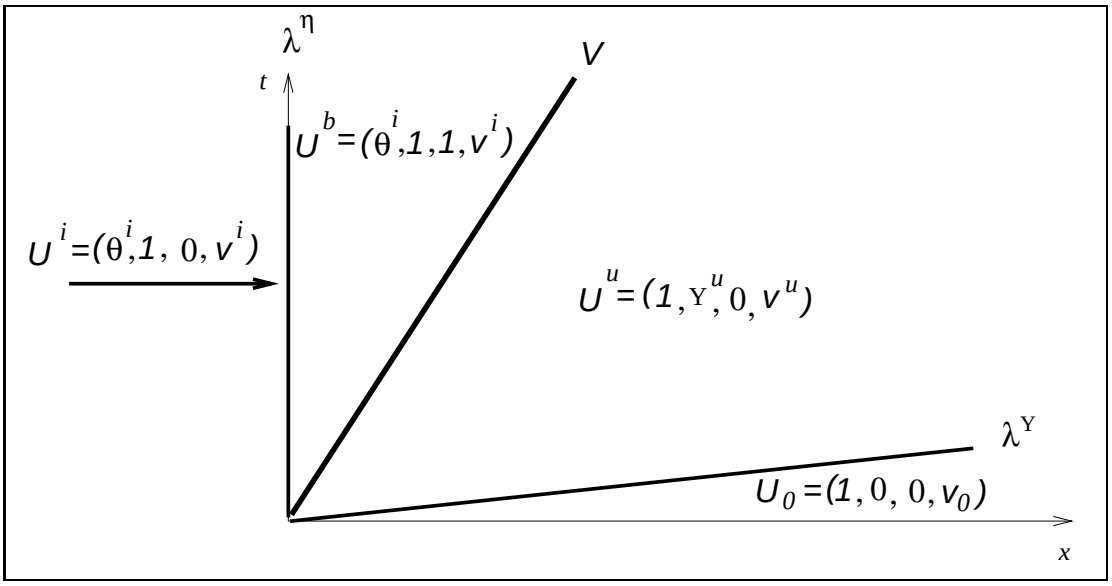

FIGURE 7.3. *Case (B.1):* Regions separated by immobile, combustion and gas composition waves. Values of θ, Y, η and v in each region.

Remark 7.5. It is easy to see that in case (A) the ratios λ^θ/V and λ^Y/V do not depend on the injection data v^i and θ^i, but only on the parameter V^u. We have that $\lambda^\theta/V \approx 10^{-1}$ and $\lambda^Y/V \approx 10^3$.

Remark 7.6. We notice that, due to the fact that the combustion and the thermal waves are very slow, it takes a long time for these waves to separate from each other, while the gas composition wave (the extremely fast wave) separates from the others immediately. This should explain why such phenomena were not observed in laboratory experiments, since it is reflects transient rather than asymptotic behavior.

Acknowledgments:
We thank José Koiller and Grigori Chapiro for their valuable contributions to this paper. We thank Beata Gundelach for her expert editorial work.

REFERENCES

[1] AKKUTLU, I.Y., *Dynamics of Combustion Fronts in Porous Media*, Ph. D. Thesis, Department of Chemical Engineering, University of Southern California, 2002.
[2] AKKUTLU, I.Y., YORTSOS, Y.C., *The Effect of Heterogeneity on In-situ Combustion: The Propagation of Combustion Fronts in Layered Porous Media*, J. Pet. Tech., June 2002.
[3] AKKUTLU, I.Y., YORTSOS, Y.C., *The Dynamics of In-situ Combustion Fronts in Porous Media*, J. of Combustion and Flame, 134, 229-247, 2003.
[4] BAILY, H.R., LARKIN, B.K., Conduction-convection in Underground Combustion, Petroleum Trans. AIME, 321-331, 1960.
[5] BENHAM, A.L., POETTMANN, F.H., The Thermal Recovery Process – An Analysis of Laboratory Combustion Data, Petroleum Trans. AIME 213: 406-408, 1958.
[6] BOBERG, T.C., *Thermal Methods of Oil Recovery*, An Exxon Monograph Series, 1988.
[7] BOUSAID, I.S., RAMEY, JR., H.J., *Oxidation of Crude Oil in Porous Media*, Soc. Pet. Eng. J. 137-148, June 1968.

[8] MOTA, J.C., MARCHESIN, D., DANTAS, W.B, *Combustion Fronts in Porous Media*, SIAM Journal on Applied Mathematics, 62, 6:2175-2198, 2002.

[9] KUMAR, M., GARON, A.M., *An Experimental Investigation of the Fireflooding Combustion Zone*, Soc. Pet. Eng. Res. Eng. 55-61, February 1991.

[10] MARTIN, W.L., ALEXANDER, J.D., DEW, J.N., *Process Variable of In-situ Combustion*, Petroleum Trans., 213:28-35, 1958.

[11] PRATS, M., *Thermal Recovery*, SPE Monograph Series SPE of AIME, 1982.

[12] PENBERTHY, W.L., RAMEY, JR., H.J., Design and Operation of Laboratory Combustion Tubes, Soc. Pet. Eng. J. 183-198, 1966.

[13] SMOLLER, J., Shock Waves and Reaction-Diffusion Equations, Springer-Verlag, 1983.

[14] WILSON, L.A., REED, R.A., REED, D.W., CLAY, R.R., *Some Effects of Pressure in Forward and Reverse Combustion*, Soc. Pet. Eng. J. 127-135, 1963.

APPENDIX A. THE INTERNAL STRUCTURE OF THE NONCOMBUSTION WAVES

A.1. **The gas composition wave.** As we have seen, across the gas composition wave only Y varies from Y^- to Y^+, while θ, η, v are constant, which we denote by $\bar{\theta}$, $\bar{\eta}$, $\bar{v}$, respectively. A constant θ in Eq. (2.9) yelds constant $\rho = \bar{\rho}$. A constant η in Eq. (2.8) is consistent with $\Phi = 0$. Thus Eqs. (2.5) and (2.7) are automatically satisfied and Eq. (2.6) becomes

$$\frac{\partial Y}{\partial t} = \frac{1}{\phi L_e}\frac{\partial^2 Y}{\partial x^2}. \tag{A.1}$$

Therefore, the gas composition wave is a diffusive wave given by the solution of Eq. (A.1) with initial condition $Y(x,0) = Y^-$ if $x < 0$ and $Y(x,0) = Y^+$ if $x > 0$.

A.2. **The thermal wave.** For the thermal wave we know that the shock speed λ^θ is positive, Y and η are constant across it, $Y = \bar{Y}$, $\eta = \bar{\eta}$, and θ, v vary respectively from θ^- to θ^+ and from v^- to v^+. Since η is constant, from Eq. (2.8) we obtain that $\Phi = 0$.

For constant Y and $\Phi = 0$, Eqs. (2.6) and (2.7) are equivalent. Let us keep Eq. (2.7) with zero right hand side. Then substituting Eq. (2.9) in Eq. (2.5), the system (2.5)-(2.9) is reduced to

$$\frac{\partial \theta}{\partial t} + \frac{\partial (av)}{\partial x} = \frac{\partial^2 \theta}{\partial x^2}, \tag{A.2}$$

$$\phi\frac{\partial \theta^{-1}}{\partial t} + \frac{\partial (\theta^{-1} v)}{\partial x} = 0. \tag{A.3}$$

In Eq. (A.2), the value of a is very small (10^{-3} according to Table I) Thus we will neglect the term containing a. This is certainly a good approximation for very large times, up to $t \approx v/a$. With this approximation, Eq. (A.2) becomes a heat equation, which can be readily solved with boundary condition $\theta(0,t) = \theta^-$ and initial condition $\theta(x,0) = \theta^+$ if $x > 0$.

Now we substitute the obtained solution $\theta(x,t)$ of Eq. (A.2) in Eq. (A.3). Integrating the resulting equation for a fixed value of t, from $x = -\infty$ to x, and using the boundary conditions that $v(0,t) = v^-$ and $v(x,t) = v^+$ as $x \to \infty$, we obtain the solution $v(x,t)$ of Eq. (A.3).

Thus the thermal wave consists of a contact wave with diffusive profile.

A.3. **The fuel wave.** As we know, across this wave the temperature, gas composition, and velocity remain constant: $\theta = \bar{\theta}$, $Y = \bar{Y}$, $v = \bar{v}$ and η varies from η^- to η^+.

Constant temperature implies constant density, $\rho = \bar{\rho}$ from Eq. (2.9). Constant temperature θ, density ρ, and velocity v imply $\Phi = 0$ from Eq. (2.5) and Eq. (2.7). From Eq. (2.8) it follows $\partial\eta/\partial t = 0$, which means that the standing wave is in fact a sharp discontinuity.

Appendix B. The internal structure of the combustion wave

For convenience, by rescaling x, we rewrite the system (4.13)-(4.15) multiplied by $\theta^u V^u = \theta^u \phi V / v^u$:

$$\frac{d\theta}{dx} = a\left(\phi(\theta - \theta^u) - \left((\theta - \theta^u)\phi + \mu_g \theta^u \eta\theta\right)V^u\right) + V^u\theta^u\left(q\eta + (\theta^u - \theta)\right), \tag{B.1}$$

$$\frac{dY}{dx} = L_e\theta\left((\phi - (\phi + \mu_g\theta^u\eta)V^u\right)Y - \mu\theta^u V^u\eta - \phi(1 - V^u)Y^u\Big), \tag{B.2}$$

$$\frac{d\eta}{dx} = \frac{-\alpha\theta^u\phi^2}{(v^u)^2 V^u} Y(1-\eta)e^{\frac{-\gamma}{(\theta-1)}}, \quad \text{for } \theta > 1, \quad \text{and} \quad \frac{d\eta}{dx} = 0, \quad \text{for } \theta \le 1. \tag{B.3}$$

Equations (B.1)-(B.3) are the reduced system of nonlinear ODE's involving expressions dependent on the variables θ, Y and η. Let us define the quantity Λ depending on η, V^u and θ^u:

$$\Lambda = \phi - (\phi + \mu_g\theta^u\eta)V^u. \tag{B.4}$$

The Jacobian matrix of system (B.1)–(B.3) in the variables θ, Y and η, for $\theta > 1$, is

$$\begin{bmatrix} a\Lambda - V^u\theta^u & 0 & (q - a\mu_g\theta)V^u\theta^u \\ L_e\left(\Lambda Y - \mu\theta^u V^u\eta - \phi(1-V^u)Y^u\right) & L_e\theta\Lambda & -L_e\theta(\mu + \mu_g Y)V^u\theta^u \\ \frac{-\alpha\theta^u\phi^2}{(v^u)^2V^u}Y(1-\eta)e^{\frac{-\gamma}{(\theta-1)}}\frac{\gamma}{(\theta-1)^2} & \frac{-\alpha\theta^u\phi^2}{(v^u)^2V^u}(1-\eta)e^{\frac{-\gamma}{(\theta-1)}} & \frac{\alpha\theta^u\phi^2}{(v^u)^2V^u}Ye^{\frac{-\gamma}{(\theta-1)}} \end{bmatrix} \tag{B.5}$$

B.1. **Local analysis near the burned state U^b.** We consider Case (A) in (5.7) together with the boundary conditions (4.8), for which $\theta^b > \theta^u = 1$, $Y^b = 1$ and $\eta^b = 1$.

Susbtituting U^b and U^u in Eq. (B.4) we have that $\Lambda = \phi - (\phi + \mu_g)V^u \equiv \Lambda^b$ and the Jacobian matrix Eq. (B.5) turns to be:

$$\begin{bmatrix} a\Lambda^b - V^u & 0 & (q - a\mu_g\theta^b)V^u \\ L_e\left(\Lambda^b - \mu V^u - \phi(1-V^u)Y^u\right) & L_e\Lambda^b\theta^b & -L_e\theta^b(\mu + \mu_g)V^u \\ 0 & 0 & \frac{\alpha\phi^2}{(v^u)^2V^u}e^{-\gamma/(\theta^b-1)} \end{bmatrix}. \tag{B.6}$$

The characteristic values of the matrix in Eq. (B.6) are:

$$\lambda_1^b = a\Lambda^b - V^u, \qquad \lambda_2^b = \frac{\alpha\phi^2}{(v^u)^2V^u}e^{-\gamma/(\theta^b-1)} \qquad \text{and} \qquad \lambda_3^b = L_e\Lambda^b\theta^b. \tag{B.7}$$

We notice that in Case (A) in (5.7) we have V^u varying in the range in (6.3), and since $V_M^u > V_d^u = a\phi/(1 + a\phi + a\mu_g)$ (see Figs. (4.1), (4.2)), we have that $\lambda_1^b < 0$. Similarly, for V^u

varying in range (6.3) we obtain that $\lambda_3^b > 0$. On the other hand the sign of λ_2^b in (B.7) is obviously positive. Thus we have

$$\lambda_1^b < 0 < \lambda_2^b < \lambda_3^b \,,$$

which means that the repelling (unstable) manifold from U^b is two dimensional.

B.2. **Local analysis near the unburned state U^u.** We consider the boundary conditions (4.5), for which $\theta^u = 1$, $Y^u > 0$ and $\eta^u = 0$.

Substituting U^u in Eq. (B.4) we have that $\Lambda = \phi(1 - V^u) \equiv \Lambda^u$ and the Jacobian matrix (B.5) turns to be:

$$\begin{bmatrix} a\Lambda^u - V^u & 0 & (q - a\mu_g)V^u \\ 0 & L_e\Lambda^u & -L_e(\mu + \mu_g Y^u)V^u \\ 0 & 0 & 0 \end{bmatrix} \tag{B.8}$$

The matrix in (B.8) has characteristic values

$$\lambda_1^u = a\Lambda^u - V^u \,, \qquad \lambda_2^u = 0 \qquad \text{and} \qquad \lambda_3^u = L_e\Lambda^u \,. \tag{B.9}$$

We notice that for the parameter V^u in the range given in Eq. (6.3) we have

$$\lambda_1^u < \lambda_2^u = 0 < \lambda_3^u \,.$$

In conclusion, even though the mathematical analysis is not complete, there is no obstacle to the existence of a heteroclinic orbit connecting the state U^b to state U^u. If the central manifold associated to the *zero* characteristic value at the unburned state in (B.9) behaves as an atractor, then there is a real possibility of the existence of a heteroclinic connection family. If it behaves as a repeller, then we may have uniqueness of the connection and the combustion wave is precisely determined. We have also numerical evidences that confirm this tendency, but the necessary mathematical analysis is more sophisticated and lies out of the scope of this paper. It is the subject of a future work.

Appendix C. Typical values, nomenclature and constants

In Eqs. (2.5)–(2.10), we introduced the following variables and parameters

$$\hat{x} = \frac{\tilde{x}}{l^*}, \quad \hat{t} = \frac{\tilde{t}}{t^*}, \quad \theta = \frac{\tilde{T}}{\tilde{T}_{ig}}, \quad Y = \frac{\tilde{Y}}{Y_i}, \quad p = \frac{\tilde{p} - p_o}{p_{inj} - p_o}, \quad \rho = \frac{\rho_g}{\rho_g^i}, \quad v = \frac{\tilde{v}}{v^i}, \tag{C.1}$$

$$\mu = \frac{\tilde{\mu}\rho_f^o}{\rho_g^i Y^i}, \quad \mu_{pg} = \frac{\tilde{\mu}_{pg}\rho_f^o}{\rho_g^i Y^i}, \quad \mu_g = \frac{\tilde{\mu}_g\rho_f^o}{\rho_g^i}, \quad a = \frac{c_g\rho_g^i}{(1-\phi)c_s\rho_s}, \quad \Phi = Wt^*, \tag{C.2}$$

$$q = \frac{Q\rho_f^o}{(1-\phi)c_s\rho_s\tilde{T}_{ig}}, \qquad \kappa = \frac{\eta_g l^* v^i}{K(p_{inj} - p_o)}, \qquad h = \frac{\tilde{h}t^*}{(1-\phi)c_s\rho_s\tilde{T}_{ig}H}, \tag{C.3}$$

$$\alpha_s = \frac{\tilde{\lambda}}{(1-\phi)c_s\rho_s}, \quad L_e = \frac{\alpha_s}{D_M}, \quad \gamma = \frac{E}{R\tilde{T}_{ig}}, \quad \alpha = k_o Y^i p_o t_*, \tag{C.4}$$

where p_o corresponds to the initial gas pressure and is typically much larger than the pressure drop across the system.

TABLE I

Parameter	Value
q	1.0121
μ	205.8
μ_g	68.19
L_e	0.214
γ	23.69
α	0.027
a	6.13E-4
ϕ	0.3

Source: [1], [2]

TABLE II

Parameter	Value
Q	39542 kJ/kg fuel
E	$7.35*10^4$ kJ/kmole
R	8.314 kJ/kmole-K
k_o	498 kW-m/atm-kmole
$\tilde{T}_o$	373.15 K
p_o	1.0 atm.
Y^i	0.23 (kg/kg)
D_M	$2.014*10^{-6}$ m^2/s
λ	$8.654*10^{-4}$ kW/m-K
ϕ	0.3
$c_g\rho_g^i$	12.338 kJ/m^3-K
ρ_f^o	19.2182 kg/m^3
$(1-\phi)c_s\rho_s$	$2.012*10^3$ kJ/m^3-K
$\tilde{\mu}$	3.018
$\tilde{\mu}_g$	1.000

Source: [1], [2]

TABLE I. Typical values of the non-dimensional parameters for in-situ combustion
TABLE II. Typical values of the dimensional parameters for in-situ combustion